

九州工業大学学術機関リポジトリ



Title	Electroluminescence efficiency of blue InGaN/GaN quantum-well diodes with and without an n-InGaN electron reservoir layer
Author(s)	Otsuji, N; Fujiwara, Kenzo; Sheu, J.K.
Issue Date	2006-12-05
URL	http://hdl.handle.net/10228/535
Rights	Copyright © 2006 American Institute of Physics

Electroluminescence efficiency of blue InGaN/GaN quantum-well diodes with and without an *n*-InGaN electron reservoir layer

N. Otsuji and K. Fujiwara^{a)}

Department of Electrical Engineering, Kyushu Institute of Technology, Tobata, Kitakyushu 804-8550, Japan

J. K. Sheu

Institute of Electro-Optical Science and Engineering, National Cheng-Kung University, Tainan 701, Taiwan

(Received 4 July 2006; accepted 16 September 2006; published online 5 December 2006)

The temperature dependence of the electroluminescence (EL) spectral intensity has been investigated in detail between $T=20$ and 300 K at various injection current levels for a set of two blue InGaN/GaN multiple-quantum-well (MQW) light-emitting diodes (LEDs) with and without an additional *n*-doped $\text{In}_{0.18}\text{Ga}_{0.82}\text{N}$ electron reservoir layer (ERL). The radiative recombination efficiency of the main blue emission band (~ 480 nm) is found to be significantly improved at all temperature regions and current levels when the additional ERL is introduced. For high injection currents I_f , i.e., large forward bias voltages V_f , a quenching of the EL intensity is observed for $T < 100$ K for both LED structures, accompanying appearance of short-wavelength satellite emissions around 380–430 nm. Furthermore, the low-temperature intensity reduction of the main EL band is stronger for the LED without the ERL than with the ERL. For low I_f , i.e., small V_f , however, no quenching of the EL intensity is observed for both LEDs even below 100 K and the short-wavelength satellite emissions are significantly reduced. These results of the main blue emission and the short-wavelength satellite bands imply that the unusual evolution of the EL intensity with temperature and current is caused by variations of the actual potential field distribution due to both internal and external fields. They significantly influence the carrier capture efficiency by radiative recombination centers within the active MQW layer and the carrier escape out of the active regions into high-energy recombination centers responsible for the short-wavelength satellite emissions. © 2006 American Institute of Physics.

[DOI: [10.1063/1.2398690](https://doi.org/10.1063/1.2398690)]

I. INTRODUCTION

Despite the great success of blue and green light-emitting diodes (LEDs) based on InGaN quantum-well (QW) heterostructures, the origin of the very bright emission characteristics is still controversially discussed.^{1–10} A peculiar property of this material system is the observation of efficient luminescence at room temperature, although the density of misfit dislocations can be as high as 10^{10} cm^{-2} due to the large lattice mismatch between the InGaN/GaN epitaxial layers and the sapphire substrate. Therefore, we expect the existence of a particular mechanism, which is responsible for the enhancement of the radiative efficiency in the presence of a high defect density. Previous studies of the temperature-dependent electroluminescence (EL) spectral intensity in single-QW (SQW) diodes^{7,8} show that efficient capture processes of injected carriers by localized tail states within the SQW layer play an important role for the recombination efficiency between $T=180$ and 300 K. However, for $T < 100$ K, an anomalous quenching of the EL intensity is observed, which we attribute to a reduction of the vertical carrier capture rates.⁷ We have also investigated the temperature dependence of the EL intensity for a specially designed blue

InGaN/GaN multiple-QW (MQW) LED containing an additional *n*-doped InGaN electron reservoir layer (ERL).¹¹ This LED exhibits a significant improvement of the radiative efficiency in comparison with the LED without the ERL. In relation to the high luminescence efficiency under the presence of the high defect density in InGaN MQWs, Hangleiter *et al.*¹² and Hitzel *et al.*¹³ recently proposed that most of the defects in the active region can be decorated by the higher band gap materials thus blocking the carriers to be nonradiatively extinguished, leading to the improved radiative recombination in spite of the existence of high defect density. This lateral carrier blocking mechanism against defect trapping within the active quantum-well layer is involved with the emissions at short-wavelength regions. Therefore, it is interesting to seek for whether the short-wavelength satellite emissions are correlated with the main EL band when the radiative recombination efficiency is significantly changed as a function of temperature and bias due to the changes of carrier capture efficiency by the radiative recombination centers.

In this paper, we report on a detailed investigation of the EL intensity of InGaN/GaN LEDs with and without the ERL as a function of temperature and injection current level to study how the carrier capture efficiency varies with bias conditions. By comparing the temperature-dependent EL charac-

^{a)}FAX: +81-93-884-0879; electronic mail: fujiwara@ele.kyutech.ac.jp

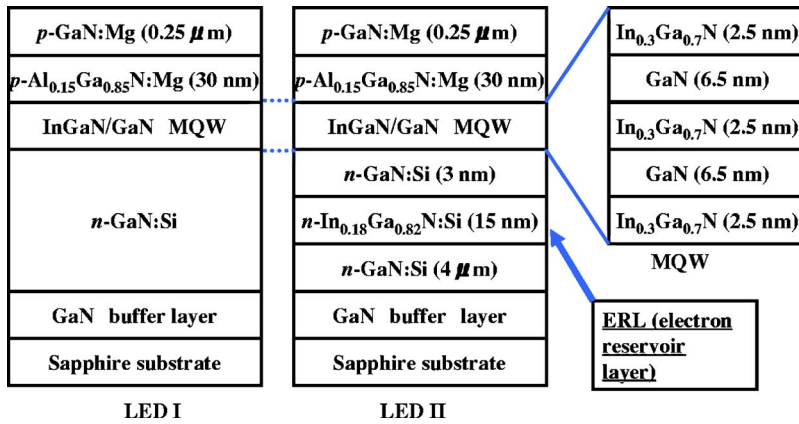


FIG. 1. (Color online) Schematic layered structure of the InGaN/GaN MQW-LEDs without (LED I) and with an additional n -type $\text{In}_{0.18}\text{Ga}_{0.82}\text{N}$ ERL (LED II).

teristics of the two MQW-LEDs for low and high injection currents over a wide spectral range, the enhanced EL efficiency observed in the MQW-LED with the ERL is attributed to an improved electron capture by radiative recombination centers. This capture is significantly influenced by the applied forward bias conditions (external field effects). Good correlation between the main EL efficiency and the short-wavelength satellite emission band is obtained.

II. EXPERIMENT

A set of two InGaN/GaN MQW-LEDs without and with an additional n -doped $\text{In}_{0.18}\text{Ga}_{0.82}\text{N}$ electron reservoir layer (ERL), named LED I and LED II, respectively, were grown by metal-organic vapor-phase epitaxy.¹⁴ A schematic layered structure of the LEDs is shown in Fig. 1. The emission region of the LEDs consists of a triple $\text{In}_{0.3}\text{Ga}_{0.7}\text{N}$ QW with a nominal width of 2.5 nm separated by 6.5 nm GaN barriers. This MQW layer is clad by 4 μm n -GaN and 30 nm p - $\text{Al}_{0.15}\text{Ga}_{0.85}\text{N}$ layers. A 15-nm-thick n -doped ($\sim 10^{19} \text{ cm}^{-3}$) $\text{In}_{0.18}\text{Ga}_{0.82}\text{N}$ ERL is located between the n -GaN clad and the active MQW layer. A thickness of n -doped GaN barrier between the ERL and the active layer is thinned to be 3 nm. The p - i - n diode is formed by forming metal contacts on 0.25 μm p -GaN cap layer and the n -GaN clad layer laterally.¹⁴ Thus, in this set of two diodes (LED I and II), only the addition of the ERL between the active MQW and the n -GaN barrier layers is different. EL spectra of the MQW-LEDs mounted on a Cu cold stage of a closed-cycle He cryostat were recorded for the dominating blue MQW emission band as well as for high-energy bands from other layers by conventional lock-in detection techniques at temperatures between 20 and 300 K as a function of the injected current between 1.0 and 50 mA.

III. RESULTS AND DISCUSSION

The current-voltage (I_f - V_f) characteristics of LEDs I and II have been measured between $T=20$ and 300 K. Figure 2 shows representative I_f - V_f curves at 20, 140, and 300 K. At 300 K, a typical V_f value for $I_f=10$ mA for LED II is 2.9 V, while for LED I the corresponding value of V_f is 3.6 V, so that a smaller V_f is necessary to achieve the same value of I_f for LED II with the ERL than for LED I without the ERL. That is, the forward bias voltage to get a certain current level is significantly reduced for LED II. This means that the stan-

dard Shockley recombination theory¹⁵ needs to be modified by the additional heterostructure configuration. When the lattice temperature is decreased to 20 K, the I_f - V_f characteristics also change significantly, and the forward bias to obtain a current level increases substantially probably due to the reduced density of holes because of trapping by the deep Mg acceptor level. That is, there are fewer holes in the p -type region at lower temperatures than at room temperature. At 20 K, the difference between the values of V_f for the two LEDs becomes even larger. When the temperature is decreased from 300 to 20 K in Fig. 2, the forward bias to achieve a sufficient current level, say 10 mA, is increased by about 2–3 V in both LEDs. This increase of the forward bias with decreasing temperature is most probably due to the reduced hole conductivity in the p -GaN and p -(Al,Ga)N layers at lower temperatures. In addition, we find a clear difference in the slope of the logarithm of I_f as a function of V_f between the two samples as well as between room and low temperatures (not shown here). Further investigations are necessary to fully understand the observed temperature dependence of the I_f - V_f characteristics and the different behaviors of the two LEDs. It should be noted, however, that the trapping of holes at 20 K due to the deep Mg acceptor level (~ 170 meV) in p -GaN cannot explain all the observed

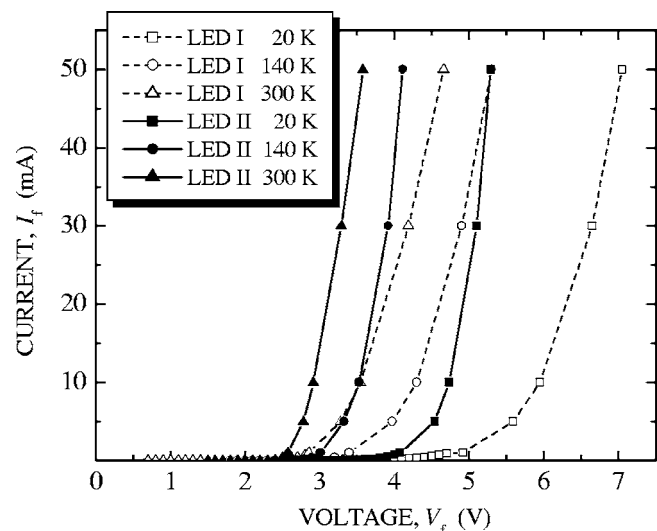


FIG. 2. I_f - V_f curves at 20, 140, and 300 K of the InGaN/GaN MQW-LEDs without (LED I: open symbols) and with an additional n -type $\text{In}_{0.18}\text{Ga}_{0.82}\text{N}$ ERL (LED II: full symbols).

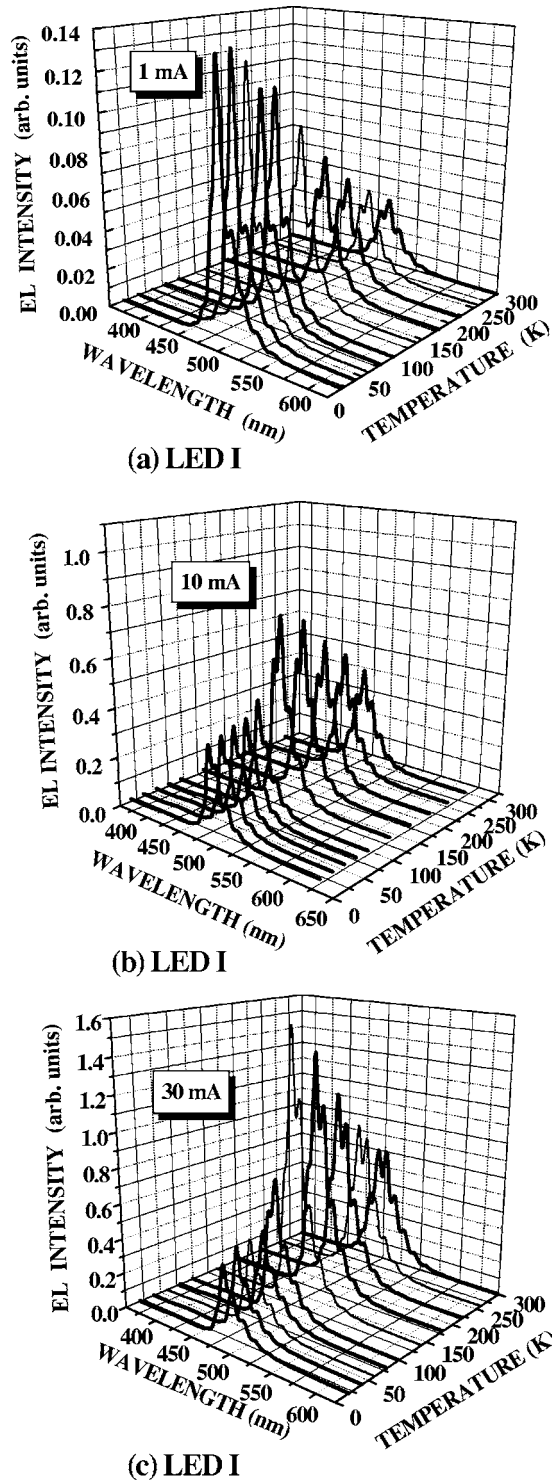


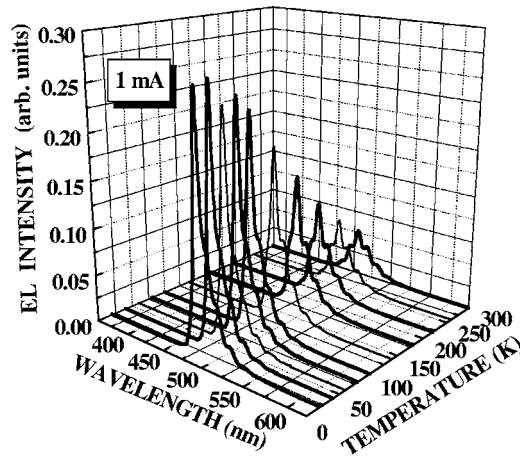
FIG. 3. Temperature-dependent EL spectra of LED I without an additional ERL for (a) $I_f=1$ mA, (b) 10 mA, and (c) 30 mA.

changes between LED I and LED II, since the p -GaN and p -(Al,Ga)N layers (with hole concentrations of $\sim 10^{17}$ cm $^{-3}$) are nominally identical in both samples. Here, we would like to emphasize that the addition of a wide n -In $_{0.18}$ Ga $_{0.82}$ N layer between the n -GaN barrier and the MQW layer has a significant impact on the I_f - V_f characteristics, i.e., it reduces V_f for a particular value of I_f .

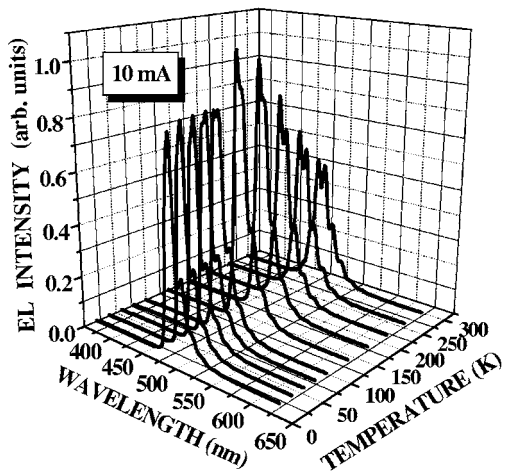
Figure 3 shows EL spectra of LED I without the ERL as a function of temperature at three injection current levels: (a)

1.0 mA, (b) 10 mA, and (c) 30 mA. The EL spectra exhibit intense emission around 480 nm with additional fine structures due to Fabry-Pérot interference fringes. When the injection current level is low at 1.0 mA in Fig. 3(a), the leading EL band exhibits the highest intensity at 20 K, and the EL peak intensity decreases as the temperature is increased. This decrease of the EL intensity with increasing the temperature is ascribed to an enhancement of nonradiative recombination processes, i.e., a reduction of the radiative recombination efficiency. When the current level is increased, however, the temperature dependence of the EL intensity is drastically changed, as illustrated in Figs. 3(b) and 3(c). A reduction of the EL intensity is clearly seen with decreasing the temperature below 100 K after reaching the maximum EL intensity around 140 K. At 30 mA [Fig. 3(c)] the EL intensity reduction is significant at 20 K and the difference in EL intensity between 140 and 20 K becomes larger than at 10 mA [Fig. 3(b)]. The similar temperature dependence of EL spectra is plotted in Fig. 4 for LED II with the ERL. At 1.0 mA [shown in Fig. 4(a)] the EL intensity observed as a function of temperature shows the similar behavior as the LED I, that is, the reduction of EL intensity with increasing the temperature. The maximum of the spectrally integrated EL intensity is reached at 20 K in Fig. 4(a). This enhancement of the radiative recombination efficiency around 20 K is commonly observed for both types of LEDs, which is similar to the photoluminescence (PL) efficiency enhancement observed at low temperatures due to the reduced nonradiative recombination.^{5,10} However, it is important to note that the absolute EL intensity for LED II becomes larger than that for LED I for all temperatures (note the ordinate scale change). When the injection current level is increased to 10 mA, the difference in EL temperature dependence between LED I and LED II becomes even larger. That is, the EL reduction with decreasing temperature is strongly suppressed at 10 and 30 mA in Figs. 4(b) and 4(c) in comparison with Figs. 3(b) and 3(c). The LED II with the ERL always shows a stronger EL intensity than LED I without the ERL, in agreement with our previous results.^{11,14}

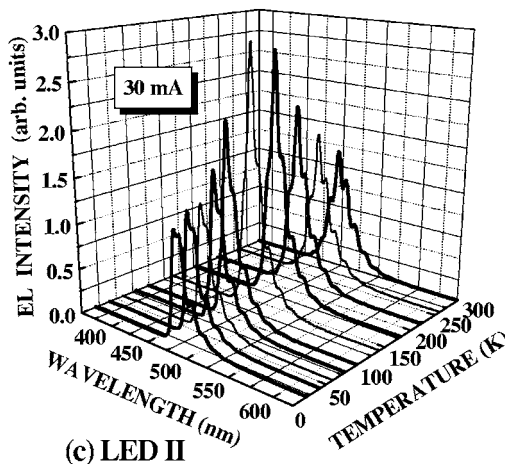
In order to further investigate the origin of the reduced EL efficiency at lower temperatures and higher injection levels, we have also evaluated the spectrally integrated EL intensity divided by the current, that is, the EL external quantum efficiency as a function of temperature for different injection current levels. Figures 5(a) and 5(b) show the integrated EL intensity as a function of temperature at various current levels from 1.0 to 50 mA (normalized to the case of 10 mA) for LED I and LED II, respectively. For $I_f=1.0$ mA, the EL efficiency exhibits its highest value at 20 K, which monotonously decreases with increasing temperature in both cases. When the injection level is increased to 10 mA, the EL efficiency per injection current decreases in comparison with the case of $I_f=1.0$ mA. Note that the EL efficiency effectively decreases with increasing current level up to 50 mA for both LEDs. Therefore, we conclude that the reduction of V_f for LED II in comparison with LED I (cf. Fig. 2) plays an important role in the enhancement of the EL efficiency at 20 K. We emphasize that the EL efficiency per injected carrier is highest at the lowest current of 1.0 mA at



(a) LED II



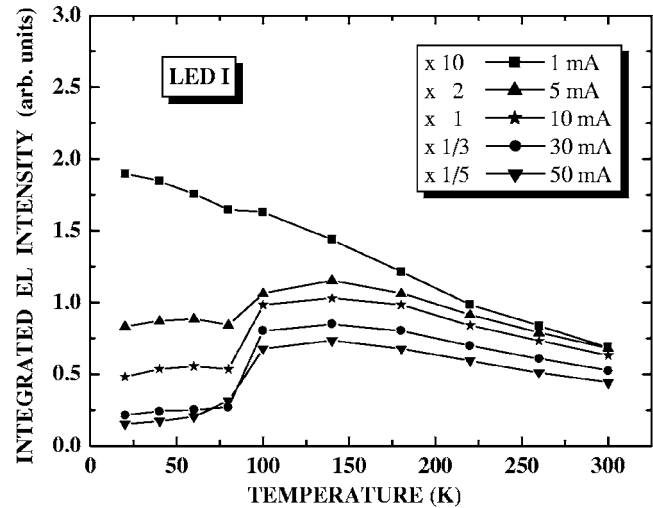
(b) LED II



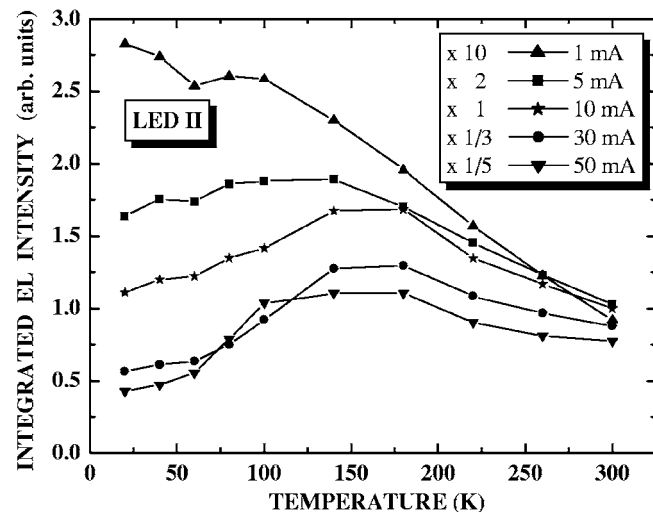
(c) LED II

FIG. 4. Temperature-dependent EL spectra of LED II with an additional ERL for (a) $I_f = 1$ mA, (b) 10 mA, and (c) 30 mA.

all temperatures in Fig. 5 for both of the diodes. It appears that the carriers are effectively captured by active centers in the MQW under the application of lower forward biases. But, applying higher forward biases, they are rather transferred to nonradiative recombination centers as a result of escape from the MQW region, thus reducing the EL efficiency. This is because the carriers can escape out of the well region due to the internal field effects, since the junction field



(a)



(b)

FIG. 5. Temperature dependence of integrated EL intensity of (a) LED I without and (b) LED II with an additional ERL for $I_f = 1, 10, 30$, and 50 mA.

direction is opposite to the internal field. We also note that the higher field existing in the well under the higher forward bias decreases the radiative recombination rate due to the quantum-confined Stark effect, which also causes the reduced EL intensity.

In Fig. 5, it is noted that the difference in the EL intensity between the two LEDs becomes even larger at 20 K for $I_f = 30$ mA than for $I_f = 1.0$ mA (cf. also Figs. 3 and 4). The difference of a factor of about 2 is seen between the EL intensities in Figs. 3(a) and 4(a) as well as in Figs. 3(c) and 4(c). For $I_f = 1.0$ mA the ratio of the EL intensities of LED II to LED I is approximately temperature independent. But it strongly increases with decreasing temperature for $I_f = 30$ mA. In order to demonstrate this difference more clearly, the ratio of the integrated EL intensity of LED II to LED I is plotted in Fig. 6 for $I_f = 1.0, 10, 30$, and 50 mA as a function of temperature. Note that the EL intensity of LED II is always stronger than that of LED I, irrespective of temperature and current level. Furthermore, the enhancement of

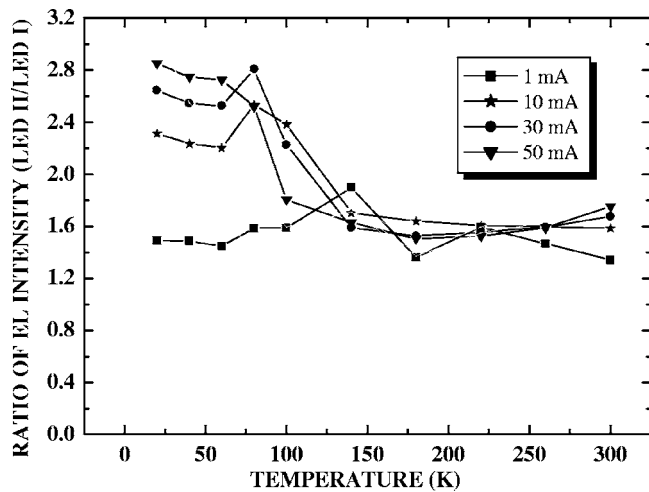


FIG. 6. Temperature dependence of ratio of integrated EL intensity (LED II/LED I) for $I_f=1, 10, 30$, and 50 mA.

the EL efficiency with decreasing temperature (around 20–80 K) is significant for LED II over LED I. The improvement of the EL efficiency for LED II with the ERL is, in fact, remarkable, indicating the importance of the carrier escape processes from radiative recombination centers in the InGaN MQW layer under the presence of higher forward biases.

In order to verify the carrier escape from the active MQW layer to the barrier regions, we have measured short-wavelength EL spectra around 360–450 nm below the leading blue (~ 480 nm) EL band including the spectral regions of the barrier materials and the ERL. The results are shown in Fig. 7 for LED I [(a) and (b)] and for LED II [(c) and (d)] at low (1.0 mA) and high (10 mA) currents, respectively. In Fig. 7(a) for LED I and at 1.0 mA, more than 100 times weaker emissions are seen at short-wavelength regions [peaked around 420 nm (2.95 eV)] than the main blue (~ 480 nm) band. The intensity of the satellite EL band monotonously increases with decreasing temperature, while the main EL band shows appreciable increases in intensity at 1.0 mA. Therefore, the results in Fig. 7(a) are explained by the fact that the EL efficiency is basically determined by the internal quantum efficiency due to the reduced nonradiative recombination processes. When the current is increased to 10 mA in Fig. 7(b), however, the EL intensity of satellite emissions drastically increases by almost one order of the magnitude relative to the main band and more rapidly increases when decreasing temperatures below 100 K. The EL efficiency of the main blue band thus decreases at 20 K when the current increases, as indicated in Fig. 5(a). That is, the main EL peak intensity decreases at temperatures below 140 K when the current is higher than 10 mA. On the other hand, as shown in Figs. 7(c) and 7(d), the short-wavelength satellite band of LED II is found to be much weaker than that of LED I. Enhancement of the satellite emission with increasing the current to 10 mA is not so significant in Fig. 7(d), indicating the improved carrier capture efficiency by the active region. This result is consistent with the improved radiative recombination efficiency in Figs. 4(b) and 4(c), es-

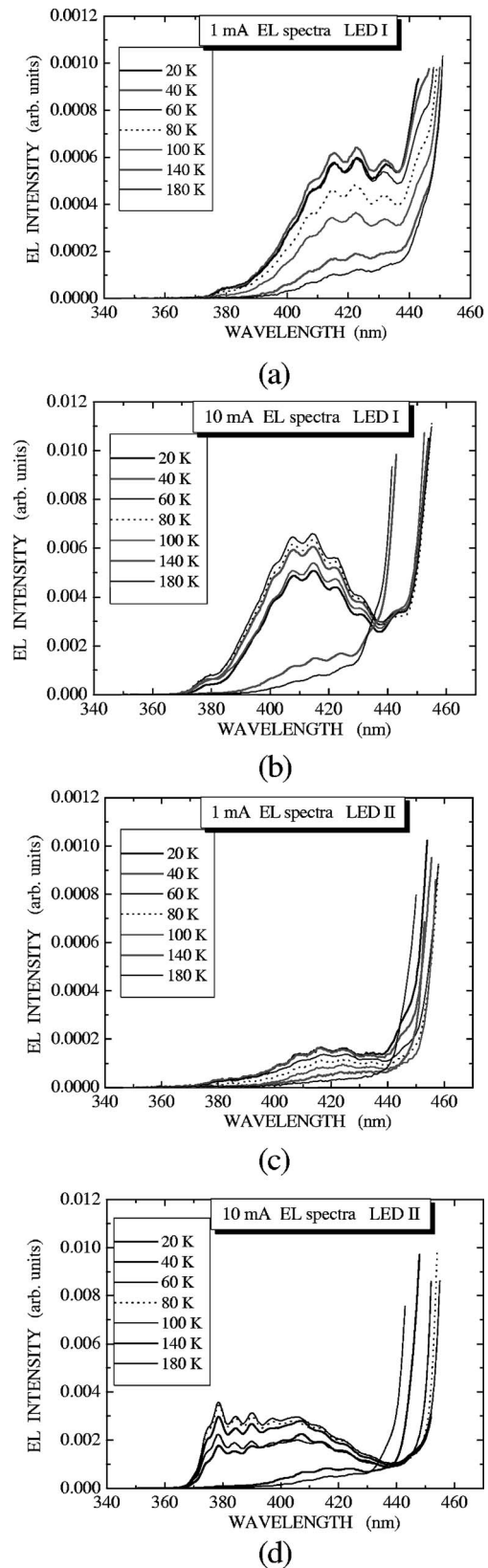


FIG. 7. Short-wavelength EL spectra of [(a) and (b)] LED I without and [(c) and (d)] LED II with an additional ERL for $I_f=1$ and 10 mA, respectively.

pecially at lower temperatures. But it is worth to note that the satellite EL emission also rapidly increases below 100 K in Fig. 7(d) in a similar way as in Fig. 7(b).

Figure 8 shows the satellite EL emission efficiency by

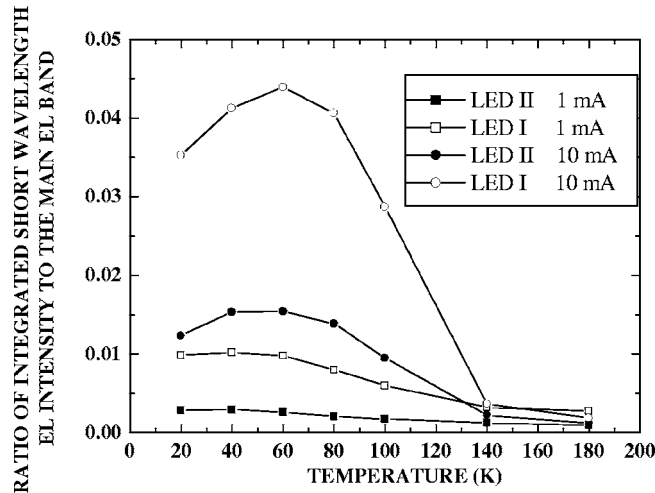


FIG. 8. Temperature dependence of ratio of the integrated short-wavelength EL intensity to the main EL band of LED I without and LED II with an additional ERL for $I_f=1$ and 10 mA.

plotting ratio of the integrated short-wavelength EL intensity divided by the integrated main EL intensity for LED I and II at low (1.0 mA) and high (10 mA) current levels as a function of temperature. For the injection current of 10 mA the short-wavelength emission efficiency of LED I is, in fact, increased at lower temperatures (below 100 K), indicating a reduction in the carrier capture rates by the MQW layer.¹¹ For LED II this increase of the satellite emission at 10 mA is significantly reduced and therefore the EL efficiency is improved due to the increased carrier capture efficiency. We note in Figs. 7 and 8 that, as the temperature goes down to 20 from 60 K, the short-wavelength satellite EL intensity slightly decreases. This is especially true for the injection current of 10 mA, while the main EL band is decreasing. We attribute these simultaneous intensity decreases of the main and satellite EL bands at 20 K to the reduction of the carrier injection efficiency from the clad layers into the active/barrier regions due to the decreased carrier mobility (most probably due to the decreased hole mobility).

In Fig. 7 the broad satellite EL band at short wavelengths around 370–430 nm (2.88–3.35 eV) is definitely enhanced under the higher forward bias conditions. It is important and interesting to inquire what the origin of this broad EL band is and whether the satellite band is related to the short-wavelength PL band (3.0–3.3 eV) observed by Hitzel *et al.*¹³ for the high-band-gap material, effective as the carrier blocking layer against defect trapping. In our analysis the EL efficiency of the satellite band, which sensitively changes with bias and temperature, is simply used as a measure for the carrier escape out of the active regions in the MQW layer. Since our observation shows that the satellite EL band is significantly suppressed by the addition of ERL, electrons injected from the *n*-type ERL are more efficiently captured into the active regions under the forward bias conditions. This is because the band gap energy of the ERL material (estimated to be ~ 3.06 eV by a sharp PL peak observed) is lower than the GaN barriers (3.5 eV), so that the carrier overshoot is suppressed, thus enhancing the main blue EL band. One possibility for those overshooting electrons with-

out the ERL is that they are to be captured in the *p*-GaIn cap layer. Thus, the satellite emissions might be due to the donor-acceptor (D-A) pairs in the *p*-GaIn cap layer. However, the broad (the bandwidth ~ 0.47 eV) satellite emission band and the large Stokes shifts (0.15–0.62 eV) observed are not consistent with the D-A recombination, as pointed out by Yang *et al.*¹⁰ As a matter of fact, the satellite EL band is enhanced with increasing the forward bias and without the ERL. So, this emission band should not be related to the InGaIn alloy fluctuations in the well layers (because the alloy effects are the same for both samples), but rather related to the barrier GaN layers. It is interesting to point out that the thinner sidewall quantum well as observed by transmission electron microscope¹² may also contribute to the stronger radiative recombination at the short-wavelength EL band. The observed broad linewidth for the satellite EL band may be explained if we take the quantum-confined Stark effect (QCSE) due to the internal field under the forward bias into account. However, more work is obviously necessary to elucidate the detailed carrier escape mechanisms under the forward bias conditions. Nevertheless, it is clear that the carrier capture by the MQW active regions is significantly improved by the additional ERL and by reducing the forward bias voltage, thus enhancing the EL efficiency by current injection.

IV. CONCLUSION

The EL spectral intensity of the main blue and the short-wavelength satellite bands has been investigated as a function of temperature and injection current for a set of two $\text{In}_{0.3}\text{Ga}_{0.7}\text{N}/\text{GaIn}$ triple-quantum-well light-emitting diodes without and with an additional *n*-doped $\text{In}_{0.18}\text{Ga}_{0.82}\text{N}$ electron reservoir layer. We find that the temperature variation of the EL efficiency critically depends on the injection current level and the presence of the additional ERL. For low current levels and thus small forward bias voltages, EL quenching does not occur below 100 K due to efficient carrier capture, as evidenced by the reduced satellite EL band. However, for high injection current levels and thus large forward bias voltages, the EL quenching persists below 100 K, and its temperature variation is more pronounced in the LED without the ERL. This unique temperature dependence of the EL intensity variation at different injection levels originates from the difference in the forward bias voltage. Appearance of the short-wavelength satellite band when the main blue emission band is reduced is consistent with the EL mechanism by Hangleiter *et al.*¹² and Hitzel *et al.*¹³ These results imply that the unusual evolution of the EL efficiency with current level and temperature can be caused by variations of the potential field distribution due to both internal and external fields, which significantly influence the carrier capture efficiency within the MQW active layer.

ACKNOWLEDGMENTS

The authors would like to thank H. Kostial, U. Jahn, and H. T. Grahn of Paul-Drude Institute for Solid State Electronics in Berlin, Germany for sample wiring and useful discussion. They also thank Y. Takahashi, H. Katou, and A. Satake for their experimental assistance. This work was supported in

part by the Grant-in-Aid for Scientific Research from the Ministry of Education, Culture, Sport, Science, and Technology of Japan under the Contract No. 16360157.

- ¹S. Nakamura and G. Fasol, *The Blue Laser Diode* (Springer-Verlag, Berlin, 1997).
- ²S. Nakamura, M. Senoh, N. Iwasa, S. Nagahama, T. Yamada, and T. Mukai, Jpn. J. Appl. Phys., Part 2 **34**, L1332 (1995).
- ³T. Takeuchi, S. Sota, M. Katsuragawa, M. Komori, H. Takeuchi, H. Amano, and I. Akasaki, Jpn. J. Appl. Phys., Part 2 **36**, L382 (1997).
- ⁴T. Mukai, K. Takekawa, and S. Nakamura, Jpn. J. Appl. Phys., Part 2 **37**, L839 (1998).
- ⁵Y. Narukawa, Y. Kawakami, S. Fujita, and S. Nakamura, Phys. Rev. B **59**, 10283 (1999).
- ⁶K. P. O'Donnell, R. W. Martin, and P. G. Middleton, Phys. Rev. Lett. **82**, 237 (1999).
- ⁷A. Hori, D. Yasunaga, A. Satake, and K. Fujiwara, Appl. Phys. Lett. **79**, 3723 (2001); J. Appl. Phys. **93**, 3152 (2003).
- ⁸A. Hori, D. Yasunaga, A. Satake, and K. Fujiwara, Phys. Status Solidi A **192**, 44 (2002).
- ⁹X. A. Cao, S. F. LeBoeuf, L. B. Rowland, C. H. Yan, and H. Liu, Appl. Phys. Lett. **82**, 3614 (2003).
- ¹⁰C. L. Yang *et al.*, J. Appl. Phys. **98**, 23703 (2005).
- ¹¹Y. Takahashi, A. Satake, K. Fujiwara, J. K. Sheu, U. Jahn, H. Kostial, and H. T. Grahn, Physica E (Amsterdam) **21**, 876 (2004).
- ¹²A. Hangleiter, F. Hitzel, C. Netzel, D. Fuhrmann, U. Rossow, G. Ade, and P. Hinze, Phys. Rev. Lett. **95**, 127402 (2005).
- ¹³F. Hitzel, G. Klewer, S. Lahmann, U. Rossow, and A. Hangleiter, Phys. Rev. B **72**, 081309R (2005).
- ¹⁴J. K. Sheu, G. C. Chi, and M. J. Jou, IEEE Photonics Technol. Lett. **13**, 1164 (2001).
- ¹⁵E. Fred Schubert, *Light-Emitting Diodes* (Cambridge University Press, Cambridge, UK, 2005).